General Disclaimer

One or more of the Following Statements may affect this Document

- This document has been reproduced from the best copy furnished by the organizational source. It is being released in the interest of making available as much information as possible.

- This document may contain data, which exceeds the sheet parameters. It was furnished in this condition by the organizational source and is the best copy available.

- This document may contain tone-on-tone or color graphs, charts and/or pictures, which have been reproduced in black and white.

- This document is paginated as submitted by the original source.

- Portions of this document are not fully legible due to the historical nature of some of the material. However, it is the best reproduction available from the original submission.

STANFORD UNIVERSITY

DEPARTMENT OF AERONAUTICS AND ASTRONAUTICS

September 1984

Subject: Progress Report covering the period February 1984 to September 1984 on NASA Research Grant NGL-05-020-243, "Refined Methods of Aeroelastic Analysis and Optimization," Holt Ashley, Principal Investigator.

To: Mr. R.V. Doggett, Jr., NASA Langley Research Center, Technical Monitor, and NASA Scientific and Technical Information Service.

The most recent published report describing work funded by this grant is still Ref. 1, the third such product based on the Doctoral Thesis of of Nitzsche (Ref. 2). However, a paper by the Ph.D. candidate Valana Wells (Ref. 3) appears in the bound volume of the 14th I.C.A.S. Congress in Toulouse and was delivered with outstanding success by its author at that meeting. As described below for information, the Wells paper deals with a new linearized potential theory for a multi-bladed propeller in steady, subsonic flight. Travel expenses for this presentation were not furnished by NASA, nor was there an attribution to NASA because the research was supported form several sources. An extension is now planned, however, to the oscillating propeller for flutter analysis and the like; this will receive significant funding from the present grant.

Professor Ashley described some of Nitzsche's results in an invited seminar delivered at Arizona State University, Tempe, on March 30, 1984. Entitled "Vibration and Flutter of a Vertical Axis Wind Turbine Blade," this not only reviewed Nitzsche's theoretical investigation but also presented more general information about wind energy and about design problems of curved, rotating airfoils.

The September 1983 Progress Report gave some details about research undertaken last summer by the Principal Investigator and dealing with the influence on aeroelastic stability on various kinds of "strong nonlinearity." During a busy academic year and summer, there has been time only for limited progress in this effort. Accordingly, a review of the subject is postponed until a later report. The remainder of the present one focuses again on the work of Ph.D. candidate John Green. Also described is a study of subsonic propeller theory by Ph.D. candidate Wells, whose Research Assistant appointment is being partially supported by Grant NGL-243.

Activity of Graduate Student J. Green on Divergence of Laminated Composite Lifting Surfaces.

The February 1984 Progress Report outlines the early stages of the work done on the divergence of forward swept wings. This early investigation focused on isotropic structures, for which analytic solutions were available (Refs. 4, 5 and 6). The integrating matrix technique proved both accurate and quick to converge upon the known results.

The study of composite wings is well along, with comparisons being made to the work such as Blair, (Ref. 7). Blair's paper includes both computational and experimental results for composite plates, with and without an aerodynamic shell, and it is the former case that is of most direct applicability. The largest part of Blair's report deals with a composite plate with a fibreglass overlay to provide an aerodynamic shape. However, he also studies three cases with the plate alone and describes wind-tunnel tests for three fibre orientations and four sweep angles. Interestingly Ref. 7 concludes that tests done with the aerodynamic shell were unnecessarily complicated.

The integrating matrix code developed at Stanford was run with these three fibre orientation angles and a full range of forward sweep angle. The calculations are summarized in Figs. 1, 2, 3, reproduced from the last progress report. The variable fibre angle θ applies

to the two outermost fibres in the following lay-up:

$$[\mp 45/90/\mp 45/90/\mp 45/90_2/\theta_2]_s$$

The figures show that the integrating matrix results match the experimental ones very well and that they are consistently closer than those from the CWING code which Blair used. This gives encouragement for the potential usefulness of integrating matrices as a fairly simple and cheap solution technique, since the data in these figures derive from the solution only of a 4 x 4 eigenvalue problem.

The remaining Figs. 4 and 5 demonstrate two methods of displaying the behavior of composite wings with varying fibre orientations to a designer. The contour plot is more familiar, and permits more precise readings to be taken, but the three dimensional plot provides a very graphic demonstration, and is better for giving a feel for the phenomenon.

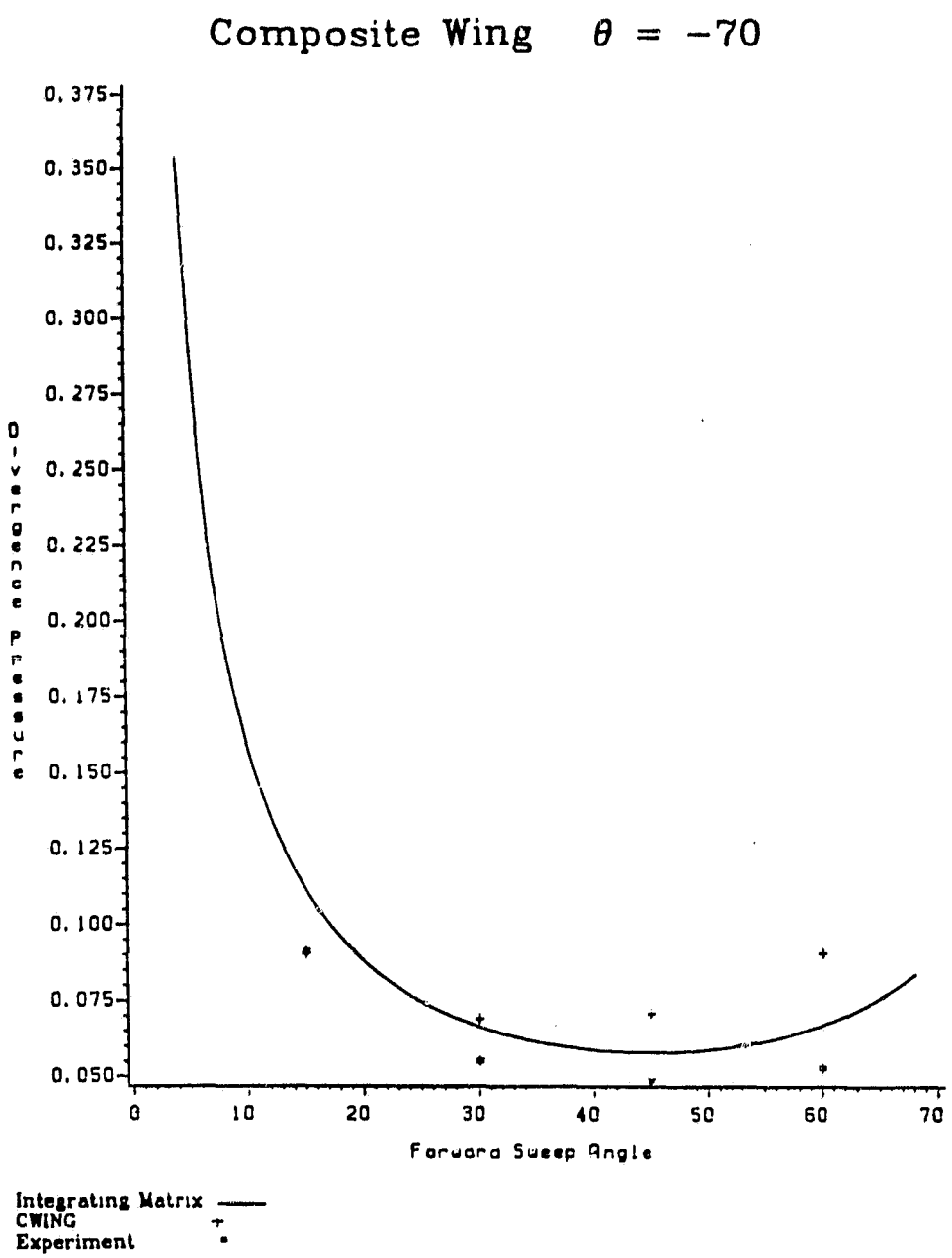

Fig. 1 — Comparison of Results with Tests of Ref. 7.

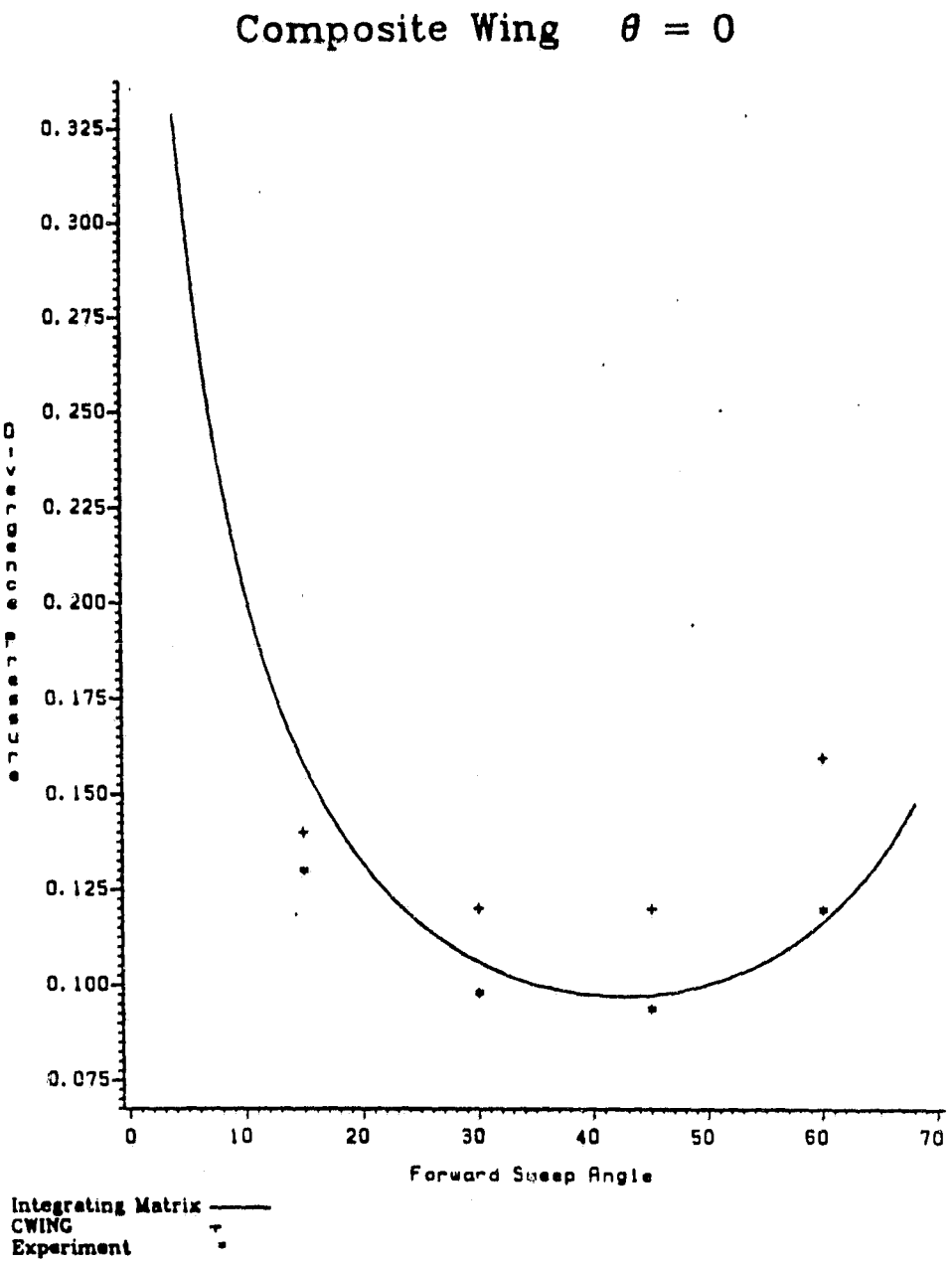

Fig. 2 — Comparison of Results with Tests of Ref. 7.

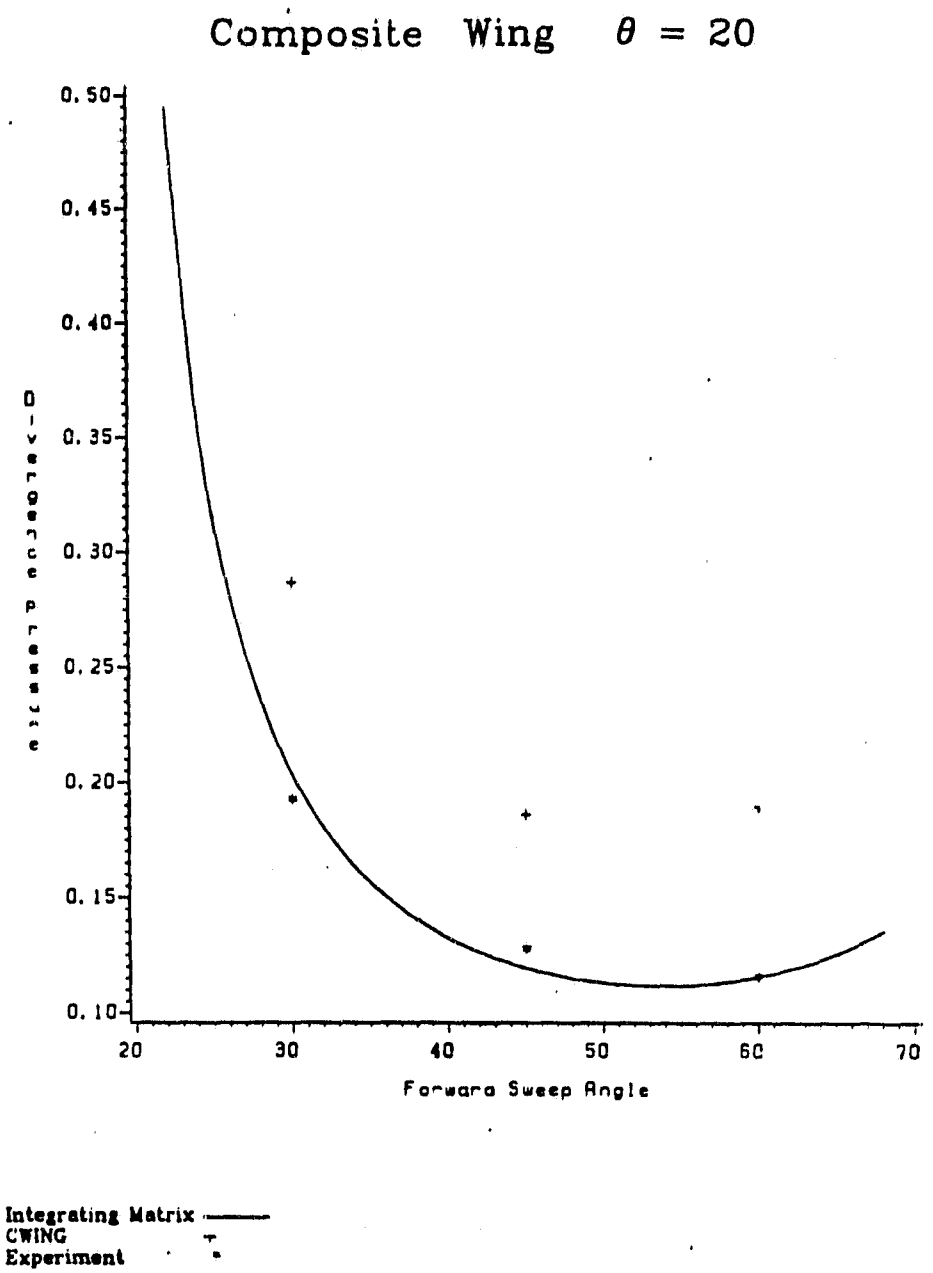

Fig. 3 — Comparison of Results with Tests of Ref. 7.

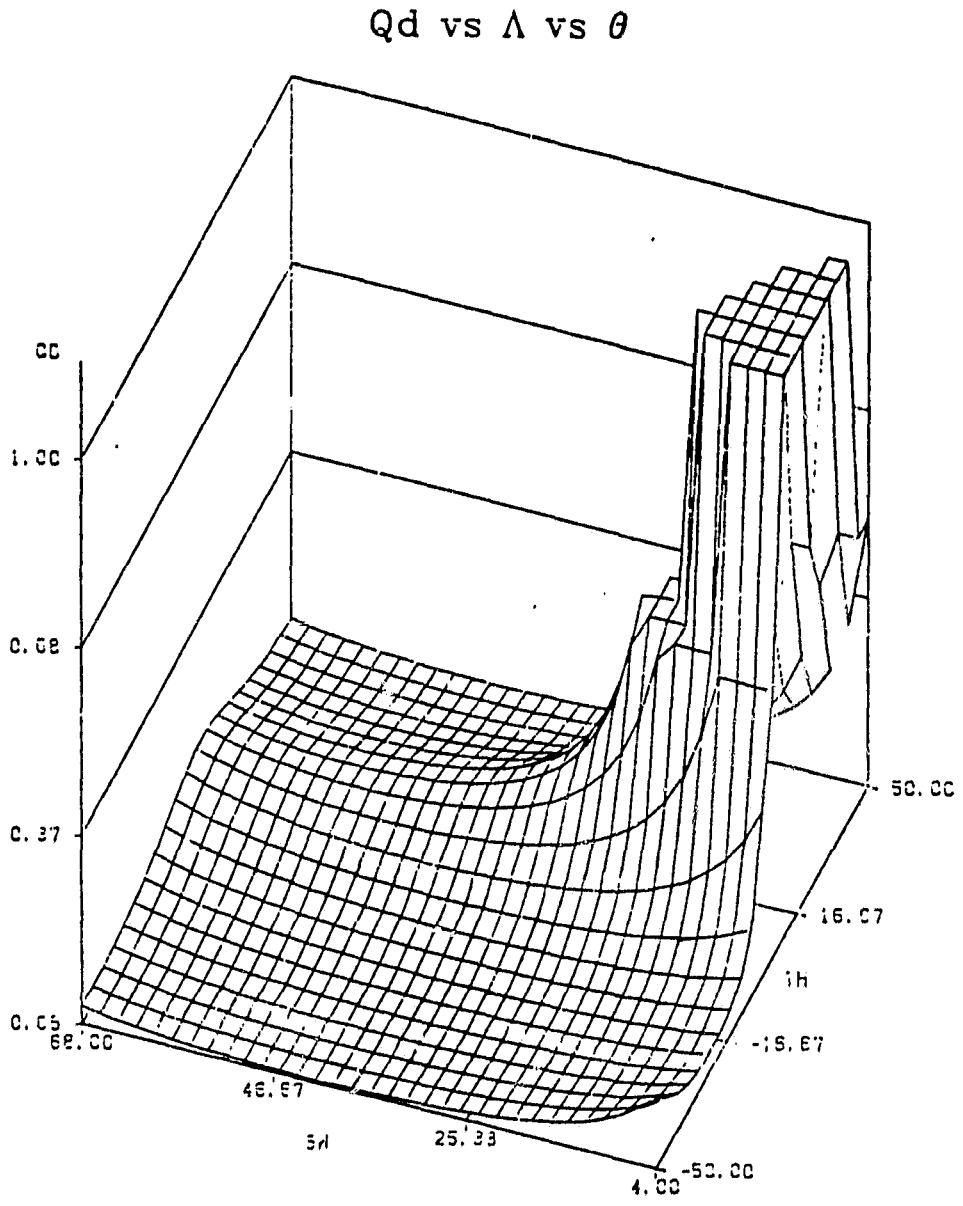

Fig. 4 — 3D Plot of Divergence Dynamic Pressure *vs* wing sweep angle and fiber orientation.

Qd vs θ vs Λ

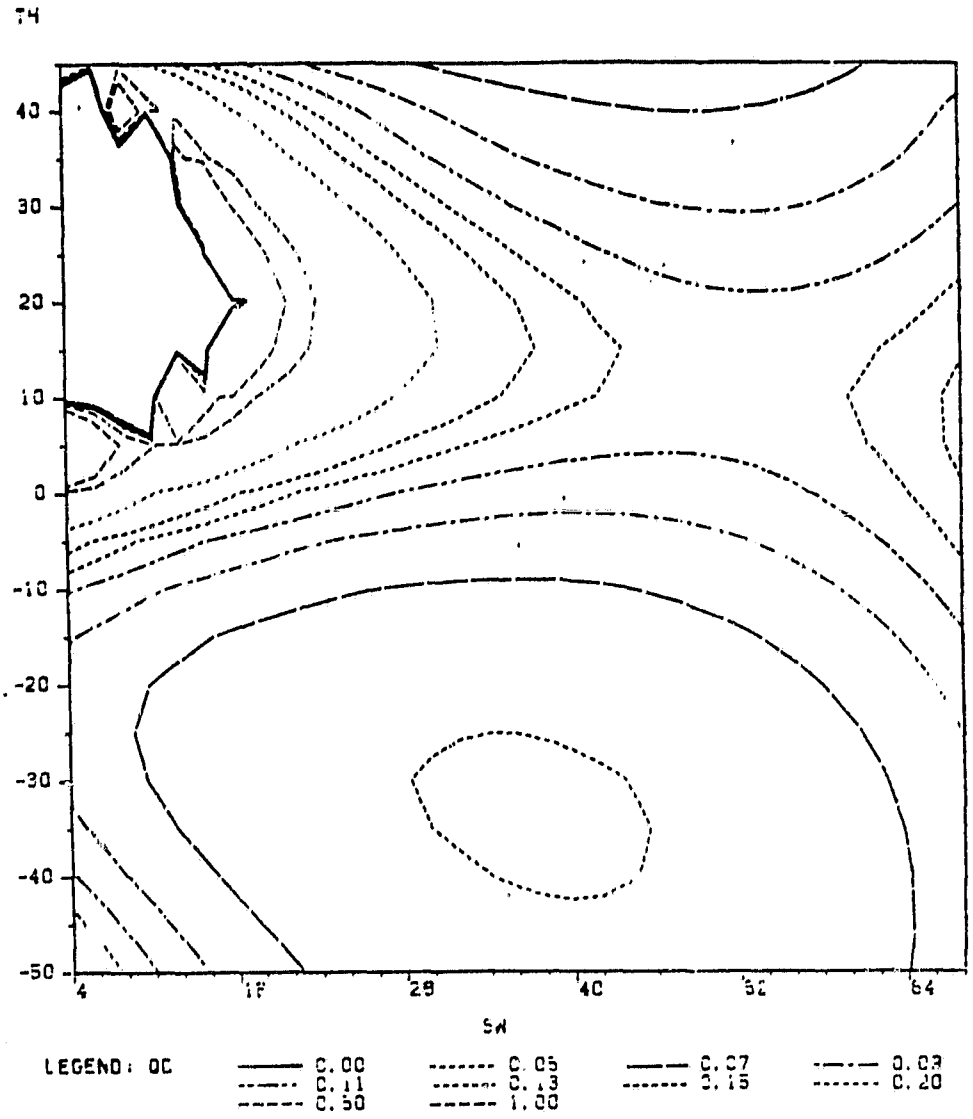

Fig. 5 — Contour Plot of Fig. 4.

Before going on to complete the study of divergence as a function of the foregoing and other parameters, it is useful to be able to evaluate the effect of flutter. Although divergence has been seen as the primary barrier to practical application of forward swept wings, the cure afforded by aeroelastic tailoring comes with a penalty. The composite layups that alleviate divergence can also reduce the flutter speed. (See for instance Refs. 8, 10 and 11.)

The aim here is to be able to modify the 3-D plot for divergence (e.g., Fig. 4) to include flutter and thus produce a general aeroelastic stability boundary. The method used to calculate the flutter speeds is based, of course, on the integrating matrix, and an outline of the relevant theory follows (Ref. 9).

The general vector equation of motion is

$$\frac{dy}{dx} = Zy + s^2My + sCy - Q(s,q)y, \tag{1}$$

where

y = state vector

Z = structural matrix

M = mass matrix

C = damping matrix

Q = aerodynamic matrix

s = Laplace variable

q = dynamic pressure

After applying the integrating matrix to both sides of the equation (1) and enforcing a cantilever boundary condition, the problem takes on the following matrix form:

$$\begin{bmatrix} (I+G_{22}) & G_{23} & G_{24} \\ G_{32} & (I+G_{33}) & G_{34} \\ G_{42} & G_{43} & (I+G_{44}) \end{bmatrix} \begin{Bmatrix} \gamma \\ w \\ \alpha \end{Bmatrix} = 0, \tag{2}$$

with

$$G = T\left[Ms^{*2} - Q(s^*,\lambda)\right] \tag{3}$$

Here

T = includes boundary conditions, structural matrix and integrating matrix

s^* = nondimensional Laplace variable

λ=nondimensional dynamic pressure

Equation (2) depends upon the two variables, and flutter is indicated when the real part of s^* becomes positive. Thus to solve (2) it is necessary to assign a value to λ and calculate the value of s^* for which the determinant is zero. This solution is done using an algorithm similar to Muller's method (Ref. 9) to find the roots of the determinant. Muller's method proves to be a very efficient and accurate approach.

Having found the root of the determinant, a check is made to see if its real part is positive. If not, a new value of λ is tested. When the real part becomes positive a further calculation can be made to evaluate the value of λ at which flutter occurs.

In order to be able to generate a 3-D carpet plot like Fig. 4 it is necessary to calculate the flutter speed of a large number of configurations. If the flutter speed has to be determined by manually testing the sign of the root then obviously much time would be wasted. Thus it is planned to develop an automatic "search" routine such as was used by Edwards (Ref. 12). He applied a gradient search algorithm with some success, and it is hoped that such a scheme will make 3-D plots feasible.

The results of the divergence calculations were compared with the experimental results of Blair (Ref. 7); however, he did not include any flutter examples. It is intended to compare the flutter calculations with the experimental work of Sherrer et.al (Ref. 8), but since all their tests were for a composite plate with an aerodynamic shell, it will be necessary to include a correction for such a shell in the integrating matrix calculations. This work is currently being undertaken.

Activity of Graduate Student V. Wells on Subsonic Propeller Theory, with a Goal of Aeroelastic Analysis

This summary of progress is based primarily on the theory and examples of Ref. 3, copies of which can be supplied if required. After reviewing past linearized solutions for incompressible and compressible flow past thin screw propellers, the work focuses on a potential flow solution in the reference frame depicted by Fig. 1 of the February 1984 Progress Report. Writing a linearized P.D.E. for the disturbance potential, the procedure converts to a non-inertial cylindrical system (r, θ, z, t) defined by

$$\begin{aligned} r &= \tilde{r}, \quad \theta = \tilde{\theta} + \omega \tilde{t} \\ z &= \tilde{z}, \quad t = \tilde{t}. \end{aligned} \tag{4}$$

Here ω is angular speed in rad./sec. Performing these coordinate transformations gives the unsteady, linearized potential equation in the rotating system:

$$\nabla^2 \varphi = M^2 \frac{\partial^2 \varphi}{\partial z^2} + 2MM_\theta \frac{1}{r} \frac{\partial^2 \varphi}{\partial z \partial \theta} + M_\theta^2 \frac{1}{r^2} \frac{\partial^2 \varphi}{\partial \theta^2} + \frac{1}{a^2} \left\{ 2U \frac{\partial^2 \varphi}{\partial z \partial t} + 2\omega \frac{\partial^2 \varphi}{\partial \theta \partial t} + \frac{\partial^2 \varphi}{\partial t^2} \right\} \tag{5}$$

where $M_\theta \equiv \frac{\omega r}{a}$ is the radially varying apparent Mach number in the angular direction.

In general, the solution to a linearized lifting body problem is subject to the following conditions:

1.) Tangency of the flow at the body surface;

2.) Vanishing (or at least finiteness) of disturbances an infinite distance away from the body and its wake; and

3.) Zero normal velocity through the wake.

The first of these conditions has the mathematical representation

$$\frac{\partial F}{\partial \tilde{t}} + \vec{V} \cdot \nabla F = 0 \text{ on } F = 0, \tag{6}$$

where $F = 0$ represents the surface of the lifting body, and $\vec{V} = \nabla\Phi$ is the total velocity vector in an inertial coordinate system. By the rule for vector time derivatives, in a non-inertial frame, the total velocity, as seen in the coordinate system rotating with angular speed, ω, is:

$$\vec{W} = \vec{V} - \vec{\omega} \times \vec{r} = \vec{V} - \omega r\hat{\theta}. \tag{7}$$

Substitution into the above boundary condition, along with the conversion of the time derivative, gives the boundary condition in the rotating reference frame:

$$0 = \frac{\partial F}{\partial t} - \omega\frac{\partial F}{\partial \theta} + \vec{W} \cdot \nabla F = \frac{\partial F}{\partial t} + \vec{W} \cdot \nabla F \text{ on } F = 0, \tag{8}$$

which is the expected result. In other words, the body boundary condition may be treated in the same manner in the rotating coordinate system as it is in the inertial system, as long as the local freestream velocity, $\vec{W}$, is considered.

The wake boundary condition can be made mathematically tractable by assuming –

1.) Unsteady perturbations are small so that the unsteady wake has, to leading order, the same shape as the steady wake; and

2.) The slipstream velocity, ω, is much smaller that the freestream velocity, U.

With these assumptions, the position of the wake can be approximated by:

$$\theta - \frac{\omega}{U}z = +(n-1)\frac{2\pi}{B}, \quad r < R, \tag{9}$$

for $B \equiv$ the number of propeller blades, $n \equiv$ the blade index, and $R \equiv$ the blade radius. For $r \equiv r_0$ and $n = 1$, for example, the equation describes a single helix with radius r_0 and origin at $\theta = 0$. The wake surface is a helicoid made up of an infinite number of these helices with radii from $r = 0$ to $r = R$ originating at $z = 0$ and at each angular station corresponding to a propeller blade location.

The first order analysis assumes that all motion of the helicoidal wake occurs in the axial direction. Since there can be no flow through the wake, the wake condition is expressed as

$$\omega \cos\epsilon = u_z \cos\epsilon - u_\theta \sin\epsilon \tag{10}$$

on

$$\theta - \frac{\omega}{U} z = (n-1)\frac{2\pi}{B}, \quad r < R \tag{11}$$

where $u_z \equiv$ induced velocity in the z–direction, $u_\theta \equiv$ induced velocity in the θ–direction, and $\epsilon \equiv$ helix angle $= tan^{-1} U/\omega r$. In terms of the velocity potential, then, the boundary condition is

$$\omega r \omega = \omega r \frac{\partial \varphi}{\partial z} - \frac{U}{r}\frac{\partial \varphi}{\partial \theta}. \tag{12}$$

Most work to date has focused on the aerodynamics of the steady propeller; that is, a rigid propeller experiencing a uniform inflow. These conditions allow the time dependent terms in equation (5) to be excluded since, now, the flow field appears steady in the rotating, translating coordinate system.

The dimensional spatial variables, r and z, have convenient dimensionless forms— $\rho = \omega r/U$ and $\bar{z} = \frac{\omega z}{U}$. Dropping the bar over the dimensionless z variable, the steady, potential equation becomes:

$$\frac{\partial^2 \varphi}{\partial \rho^2} + \frac{1}{\rho}\frac{\partial \varphi}{\partial \rho} + \beta^2 \frac{\partial^2 \varphi}{\partial z^2} + \frac{1}{\rho^2}(1 - M^2\rho^2)\frac{\partial^2 \varphi}{\partial \theta} - 2M^2 \frac{\partial^2 \varphi}{\partial \theta \partial z} = 0, \tag{13}$$

with $\beta^2 = 1 - M^2$. Equation (13) appears to depend on one parameter (M) only. However, the advance ratio parameter is hidden in the dimensionless variables, ρ and z.

In "helical" coordinates described by $\zeta = \theta - z$ and $\sigma = \theta + z$, this becomes

$$\varphi_{\rho\rho} + \frac{1}{\rho}\varphi_\rho + (1 + \frac{1}{\rho^2})\varphi_{\zeta\zeta} + (1 + \frac{1}{\rho^2} - 4M^2)\varphi_{\sigma\sigma} - 2(1 + \frac{1}{\rho^2} - 2M^2)\varphi_{\zeta\sigma} = 0. \qquad (14)$$

Goldstein (Ref. 15) shows that, in the far wake, the flow field depends only on the variables ρ and ζ. (ζ runs counter to a helix at a given radius.) This results from purely geometrical considerations, and therefore holds for both compressible and incompressible flows. Thus in the far wake,

$$\varphi_{\rho\rho} + \frac{1}{\rho}\varphi_\rho + (1 + \frac{1}{\rho^2})\varphi_{\zeta\zeta} = 0, \qquad (15)$$

which is exactly the equation solved by Goldstein. This result is of interest on two accounts:

1) The perturbed flow in the far wake has an incompressible character which implies that quantities which depend only on the far wake are invariant from incompressible to compressible flow.
2) The far wake solution for a propeller in incompressible flow also satisfies the compressible equation.

Davidson (Ref. 16) pointed out the latter and used that fact in his study of the propeller in compressible flow in a wind tunnel. This study also utilizes the far wake solution as will be shown.

The problem of compressible, potential flow about a propeller reduces to that of solving a partial differential equation Eq. (14), subject to

1. φ finite at $\rho = 0$,
2. Sommerfield radiation as ρ becomes infinite,
3. No flow through the propeller blades, and
4. No flow through the propeller wake.

The solution to the equation for the incompressible velocity potential, $\varphi_i(\rho, \theta - z)$, also solves the compressible equation. Though it cannot capture the compressible effects at the propeller blades, this solution accurately describes the far wake flow. Thus, a superposition

of a compressible solution, which accounts for effects near the blades but dies out in the far wake, on the incompressible solution also constitutes a solution to the linear differential equation. As will be shown later, the superposed solution is desirable in this case as the analytic form of the compressible solution does not lend itself well to satisfying the wake boundary condition.

Though most forms of the incompressible velocity potential, φ_i, are derived at an infinite distance behind the propeller plane, any form given as $\varphi_i(\rho, \theta - z)$ must solve Eq. (14). However, in order for the superposed solution $\varphi = \varphi_c + \varphi_i$ to form a solution to the entire problem, the sum, $\varphi_i + \varphi_c$, must satisfy the boundary conditions. The first two conditions, finite φ at $\rho = 0$ and proper dying out of the disturbance as $\rho \to \infty$, do not cause any difficulty as they can be satisfied independently by φ_i and φ_c.

In order to account for the more problematic conditions (3) and (4) above, the flow field can be artificially divided into two regions – one forward of the propeller plane in which only the compressible velocity potential holds, and the other behind the propeller plane in which both φ_i and φ_c apply. The form of φ_i, which automatically provides for the existence of a trailing wake, necessitates the division of the flow field. This division, however, requires the introduction of two more "boundary" conditions which assure continuity at the propeller plane. Designating $\varphi_c{}^+$ as the forward potential and $\varphi^- = (\varphi_i + \varphi_c{}^-)$ as that behind the propeller, and situating the propeller at $z = 0$ as before, a continuous flow field is ensured by

$$\varphi_c{}^+ \Big|_{z=0} = \varphi_i \Big|_{z=0} + \varphi_c{}^- \Big|_{z=0}, \tag{16}$$

and

$$\frac{\partial \varphi_c{}^+}{\partial z} \Big|_{z=0} = \frac{\partial \varphi_i}{\partial z} \Big|_{z=0} + \frac{\partial \varphi_c{}^-}{\partial z} \Big|_{z=0}. \tag{17}$$

Since both φ^+ and φ^- are valid at $z = 0$, both must satisfy the condition of no flow through the propeller blades.

Details of this incompressible result are worked out in Ref. 3 on the basis of Reissner's paper (Ref. 17). A general solution to the steady, compressible potential equation may be obtained through separation of variables. The resulting series solution has the form:

$$\varphi = \sum_{n=0}^{\infty} A_n R_n(\rho) Z_n(z) e^{inB\theta}; \tag{18}$$

with

$$R_n(\rho) = C_{nB}\left(\rho\sqrt{M^2n^2B^2 + \lambda_n^2}\right), \tag{19}$$

and

$$Z_n(z) = exp\left\{i\frac{nB}{\rho s^2} \pm \frac{1}{\beta}\sqrt{\lambda_n^2 - \frac{n^2B^2M^2}{\rho_s^2}}\right\} z. \tag{20}$$

C_{nB} represents a linear combination of solutions to Bessels equation, λ_n is the separation constant, or eigenvalue, and $\rho_s \equiv \beta/M$ is the dimensionless radius at which the local freestream velocity becomes sonic. Applying the boundary condition requiring finiteness of φ at $\rho = 0$ gives

$$R_n(\rho) = J_{nB}\left(\rho\sqrt{M^2n^2B^2 + \lambda_n^2}\right). \tag{21}$$

A separated solution is a slightly different form from that given above was first proposed by Busemann (Ref. 13).

The behavior of the J-Bessel function as its argument approaches infinity will cause automatic satisfaction of the radiation boundary condition. This leaves no mechanism for determining values for the eigenvalues, λ_n; in fact, the notion of the eigenvalue has no real meaning for problems of infinite domain. Therefore, the solution must be obtained using a method other than a simple separation of variables.

Due to periodicity in the angular coordinate, the expected solution to the partial differential equation has the form:

$$\varphi = \sum_{n=0}^{\infty} \varphi_n(\rho, z) e^{inB\theta} \tag{22}$$

Substituting this into the PDE gives

$$\varphi_{n_{\rho\rho}} + \frac{1}{\rho}\varphi_{n_\rho} - n^2B^2\frac{1}{\rho^2}\left(1+\rho^2M^2\right)\varphi_n = -\beta^2\varphi_{n_{zz}} + 2inBM^2\varphi_{n_z} \tag{23}$$

Performing a Hankel transform on this equation gives

$$\beta^2\bar{\varphi}_{zz} - 2inBM^2\bar{\varphi}_z - \left(\gamma^2 - n^2B^2M^2\right)\bar{\varphi} = 0, \tag{24}$$

a second order, ordinary differential equation for the Hankel-transformed potential, $\bar{\varphi}$. The Hankel parameter, γ, appears only parametrically. The solution to this equation is easily obtained:

$$\bar{\varphi}_n(z;\gamma) = A_n exp\left\{\left[i\frac{nB}{\rho_s^2} \pm \frac{1}{\beta}\sqrt{\gamma^2 - \frac{n^2B^2}{\rho_s^2}}\right]z\right\}. \tag{25}$$

Inverting this transformed solution results in

$$\varphi_n(\rho,z) = \int_0^\infty A_n(\gamma)\gamma J_{nB}(\gamma_\rho)exp\left\{\left[i\frac{nB}{\rho_s^2} \pm \frac{1}{\beta}\sqrt{\gamma^2 - \frac{n^2B^2}{\rho_s^2}}\right]z\right\}d\gamma. \tag{26}$$

The complete solution to the compressible potential equation is then

$$\varphi(\rho,z,\theta) = \sum_{n=0}^{\infty} e^{inB\theta}\int_0^\infty A_n(\gamma)\gamma J_{nB}(\gamma\rho)exp\left\{\left[i\frac{nB}{\rho_s^2} \pm \frac{1}{\beta}\sqrt{\gamma^2 - \frac{n^2B^2}{\rho_s^2}}\right]z\right\}d\gamma. \tag{27}$$

It remains to determine the unknown "constants," $A_n(\gamma)$.

A careful "matching" process described in Ref. 3 makes it possible to relate all of the required constants to the single unknown function $\Gamma(\rho)$, which is the unknown distribution of circulation along each of the identical propeller blades. Table 1 summarizes the results.

	Forward ($z \leq 0$)	Behind ($z \geq 0$)
A_0	$\frac{B}{2\pi}\frac{\beta}{2\gamma}\Gamma_0'(\gamma)$	$\frac{B}{2\pi}\frac{\beta}{2\gamma}\Gamma_0'(\gamma)$
A_n	$\frac{B}{2\pi}\frac{2(-1)^n}{nB}\frac{\Gamma_n'(\gamma)}{2}\left[-i-\frac{nB\beta}{\rho_s^2\sqrt{\gamma^2-\frac{n^2\beta^2}{\rho_s^2}}}\right]$	$\frac{B}{2\pi}\frac{2(-1)^n}{nB}\frac{\Gamma_n'(\gamma)}{2}\left[i-\frac{nB\beta}{\rho_s^2\sqrt{\gamma^2-\frac{n^2\beta^2}{\rho_s^2}}}\right]$
B_n	$-\frac{\Gamma_n'(\gamma)}{2}\left[-i-\frac{nB}{\beta\sqrt{\gamma^2-\frac{n^2\beta^2}{\rho_s^2}}}\right]$	$-\frac{\Gamma_n'(\gamma)}{2}\left[i-\frac{nB}{\beta\sqrt{\gamma^2-\frac{n^2\beta^2}{\rho_s^2}}}\right]$

Table 1— Coefficients for Compressible Velocity Potential Series

After the convergence of integrals appearing in Eqs. (26) and (27) is proved, one proceeds to apply a flow-tangency boundary condition to determine Γ. This condition may be expressed as

$$u_z \cos\epsilon - u_\theta \sin\epsilon = W\alpha \quad for \quad z, \theta \rightarrow blade, \tag{28}$$

for the simple case of uncambered, thin airfoils sections. u_z and u_θ are the perturbation velocities, achieved by differentiating the velocity potential. $u_z, u_\theta, \epsilon, W$, and α are all functions of radial position.

In the lifting line approximation, which is developed in detail, there is no blade at which to apply condition (28). Instead, the condition given by Reissner must be used. Referring to figure 6, this condition is given as

$$\alpha = \alpha_g - \frac{v_i}{W} \; at \; z \rightarrow 0, \theta \rightarrow \frac{\pi}{B}. \tag{29}$$

α_g is the geometric angle of attack, and v_i is the induced velocity perpendicular to W.

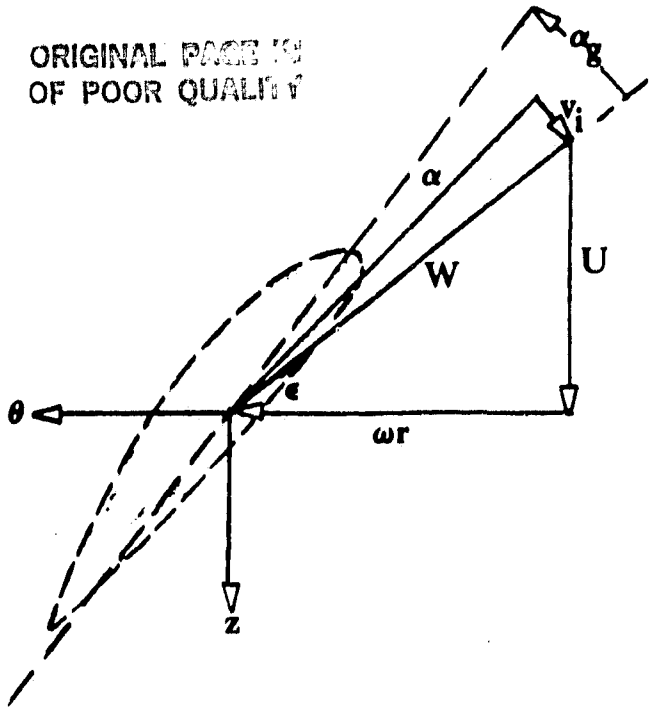

Figure 6 — Velocities at the Blade

Two well-known relations assist in reducing this to usable form: $l = \mu W \Gamma$ and $l = \frac{\mu}{2} W^2 c c_{l_\alpha} \alpha$, where $l \equiv$ lift per unit radius, $\mu \equiv$ density, $c_{l_\alpha} \equiv$ section lift curve slope and $c \equiv$ blade chord. Combining these two expression gives $\alpha = 2\Gamma / W c c_{l_\alpha}$. Substituting this into (29) gives

$$\frac{v_i}{W} + \frac{2\Gamma}{\rho_a \bar{c} c_{l_\alpha}} \frac{U}{W} = \alpha_g, \; z \to 0, \; \theta \to \frac{\pi}{B}, \tag{30}$$

where $\bar{c} \equiv c/R$, an inverse "blade aspect ration." Note that $v_i = u_z \cos\epsilon - u_\theta \sin\epsilon$, as before.

Condition (30) introduces two parameters, $\bar{c}$ and c_{l_α}. $\bar{c}$ is easily estimated for a typical propeller blade; however, c_{l_α} is not known in advance for compressible flow. It is assumed here that an estimate of c_{l_α} based on strip theory will introduce only minimal error.

By defining $\varphi^* = \frac{\omega}{U^2} \varphi$ and $\Gamma^* = \frac{\omega}{U^2} \Gamma$, Eq. (30) can be written in dimensionless form:

$$\rho \frac{\partial \varphi^*}{\partial z} - \frac{1}{\rho} \frac{\partial \varphi^*}{\partial \theta} + \frac{2\Gamma^*}{\rho \bar{c} c_{l_\alpha}} = (1 + \rho^2) \alpha_g, \; z \to 0, \; \theta \to \frac{\pi}{B}. \tag{31}$$

Carrying out and collecting the expressions for the derivatives in Eq. (31) leads to a rather complicated integral equation pair for the circulation distribution (see Eqs. (4.5 a,b) of Ref. 3). A useful method for solving these relations involves choosing a series "shape function" for $\Gamma^*(\rho)$ with unknown coefficients. Collocation at a set of K stations along the blade then yields $K \times K$ linear equations in K unknown coefficients.

The first attempt at selecting these shape functions followed a suggestion of Reissner (Ref. 17). This led, however, to difficulties with the uniformity of convergence and has been improved upon since Ref. 3 was written. At Mach Number 0.65, for example, satisfactory convergence is now attained with approximately $K = 10$ on a typical two-bladed propeller. It turns out, incidentally, that no simple "compressibility correction" can be proposed by analogy with the Prandtl-Glauert correction for steady flow over subsonic wings.

Figure 7 compares the compressible and incompressible circulation distributions for propellers with the same geometric angle of attack distribution. As expected, the compressible case has a greater magnitude of circulation, paralleling the same trend due to Mach number which occurs for straight wings.

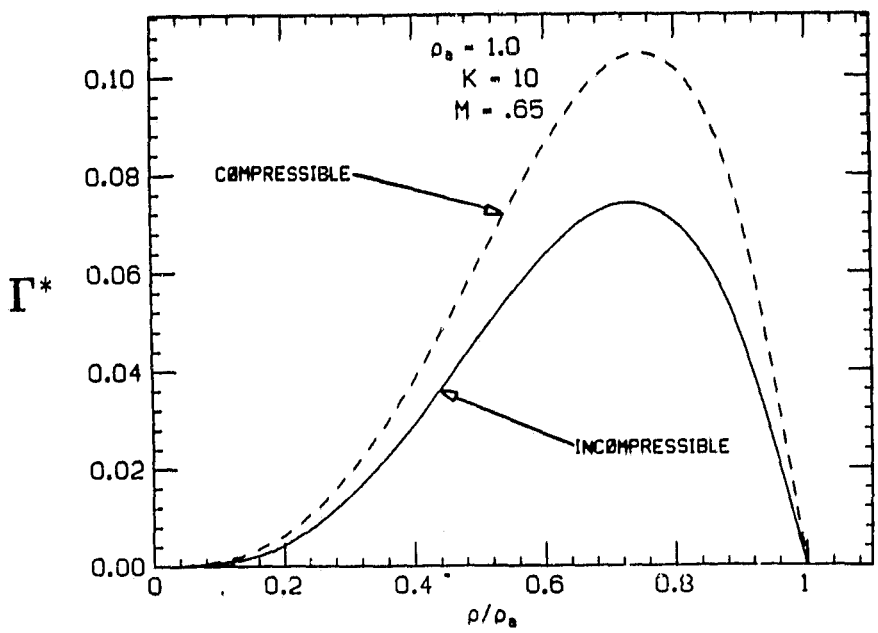

Fig 7 — Circulation Distributions

Favorable comparisons have also been made with test results on two-bladed machines, when an empirical adjustment is made to account for the profile drag of blade sections.

The results obtained inspire confidence in the derivation and the solution methods since a) they show convergence in both the series solutions for the velocities and the shape function solutions, and b) they show trends anticipated from wing theory. Of course, a favorable comparison with experiment would reinforce confidence in the method.

Further examples can be readily treated and will be shortly forthcoming. These include:

a) thrust and torque distributions,

b) efficiency calculations,

c) effects of changing Mach number and advance ratio, and

d) unsteady motions.

The Weissinger boundary condition (Ref. 18) will also be studied for accuracy improvement. In addition, a viscous drag correction term must be included to correctly predict the thrust and torque distributions, particularly for a compressible propeller analysis.

Activity of Graduate Student In Lee on Cross-Sectional Resonances of Wind Tunnels.

A limited description of this research was provided in the June 1984 continuation proposal (Ref. 18) for the present grant. Extensive details are not repeated herein. Mr. Lee's work has important implications for high subsonic flutter testing, but it has received in the past only a small amount of support from the grant. Whether it will be possible to continue this funding in the future depends, of course, upon other demands on the limited available funds and on completion dates of other student research.

It has been well known since two-dimensional analyses at NACA Langley in the 1950's and subsequent Brittish studies on 3-D cross-sections that there are various potentially-significant wall effects on the airloading of wind-tunnel models of lifting surfaces performing unsteady motions in a subsonic airstream. (In the interests of brevity, the many relevant references are not cited here.) Although transonic effects can be significant, probably

the most dramatic of these occurs when a frequency of oscillation "resonates" with a natural acoustic frequency of the tunnel cross section itself. Such "resonances" are most pronounced in closed tunnels and when the fundamental tunnel mode is involved. Effects on flutter speed of the order of 20% have been demonstrated experimentally. Thus it is desirable to be able to predict these modes and frequencies accurately.

Although the theory can be developed in a more sophisticated fashion, the key idea is that the "resonances" consist of 2-D standing waves in the cross section, with an effective speed of sound $a_\infty\sqrt{1-M^2}$. Here a_∞ is the undisturbed free-stream acoustic speed and $M < 1$ the test Mach No. It is significant that this effective speed, and the associated frequencies, become quite low as the transonic range is approached. (Ultimately, of course, nonlinearity and the formation of shocks tend to invalidate the linear potential-flow idealization.)

What Mr. Lee has succeeded in doing is to program an accurate, convergent finite-element code for finding 2-D acoustic modes of an essentially arbitrary tunnel shape. He has analyzed, for instance, the octagonal configuration of the NASA Langley TDT, discovering somewhat different natural frequencies from those previously obtained from a rectangular approximation to its shape. His program, in the original version, was capable of handling open or solid wall boundaries, along with combinations of open and solid portions that could be accomodated by the finite-element formulation. Many examples have been calculated.

Mr. Lee is currently engaged in examining porous and slotted boundaries of the sort employed in transonic facilities. Following up on some British work, he has also discovered interesting influences due to a finite plenum chamber (at constant pressure) surrounding such a transonic test section. Publications are anticipated in the near future.

REFERENCES

1. Nitzshe, F., "A Revised Version of the Transfer Matrix Method to Analyze One Di-

mensional Structures," Collected Papers, 24th AIAA Structures, Structural Dynamics and Materials Conference, Lake Tahoe, NV, May 2-4, 1983, pp. 129-136 (publication expected shortly in AIAA Journal).

2. Nitzsche, F., "Aeroelastic Analysis of a Darrieus Type Wind Turbine Blade with Troposkien Geometry," Ph.D. Dissertation, Dept. of Aeronautics and Astronautics, Stanford Univ., June 1983 (to be published, under slightly different title, as a NASA Contractor Report).
3. Wells, V., "Propellers in Compressible Flow," ICAS-84-5.6.1., Proceedings, 14th Congress of the International Council of the Aeronautical Sciences, Toulouse, France, Sept. 9-14, 1984.
4. Bisplinghoff, R. L. and Ashley, H. Principles of Aeroelasticity, Dover Publications reprint, New York, 1975. (see Chap. 7)
5. Bisplinghoff, R. L., Ashley, H., and Halfman, R. L., Aeroelasticity, Addison-Wesley Publishing Co., Reading, Mass, 1955. (see Chap. 8)
6. Dowell, E. H., *et al.* A Modern Course In Aeroelasticity, Sijthoff and Noordhoff, 1980.
7. Blair, M., "Wind Tunnel Experiments on the Divergence of Swept Wings with Composite Structures," AFWAL TR-82-3018, 1982.
8. Sherrer, V. C., Hertz, T. J. and Shirk, M. H., "A Demonstration of the Principle of Aeroelastic Tailoring Applied to Forward Swept Wings," AFWAL-TR-82-3066, 1982.
9. Lehman, L. L., "Hybrid State Vector Methods for Structural Dynamic and Aeroelastic Boundary Value Problems," Part 2 of SUDAAR 529, June 1983.
10. Hertz, T. J., Shirk, M. H., Ricketts, R. H. and Weisshaar, T. A., "Aeroelastic Tailoring with Composites Applied to Forward Swept Wings," AFWAL-TR-81-3043, 1981.
11. Shirk, M. H., Hertz, T. J. and Weisshaar, T. A., "A Survey of Aeroelastic Tailoring Theory Practice, Promise," AIAA Paper No AIAA-84-0982-CP. Proceedings 25th Structures, Structural Dynamics and Materials Conference, Palm Springs, California, 1984.

12. Edwards, J.W., "Unsteady Aerodynamic Modelling and Active Aeroelastic Control," SUDAAR 504, Stanford Univ. Dept. of Aeronautics and Astronautics, 1977.

13. Busemann, Adolf, "Theory of the Propeller in Compressible Flow," presented at Third Midwestern Conference on Fluid Mechanics (Minneapolis, Minn.), March 22-24, 1953.

14. Johansson, Bo. D. A., "Lifting Line Theory for a Rotor in Vertical Climb," Aero. Res. Inst. Sweden (FFA) Rept. 118, 1971.

15. Goldstein, S., "On the Vortex Theory of Screw Propellers," Proc. Roy. Soc. (London), Ser. A, Vol. 123, No. 792, Apr. 1929, pp. 440-465.

16. Davidson, R.E., "Linerized Potential Theory of Propeller Induction in a Compressible Flow," NACA TN-2983, 1953.

17. Reissner, H., "On the Relation Between Thrust and Torque Distribution and the Dimensions and Arrangement of Propeller Blades," Phil. Mag., Ser. 7, Vol. 24, No. 163, Nov. 1937, pp. 745-771.

18. Weissinger, J., "On the Lift Distribution of Swept Wings," translated from the German as NACA T.M. 1120, 1947.

19. Ashley, H., Principal Investigator, Proposal for the continuation of research under NASA NGL 05-020-243, "Refined Methods of Aeroelastic Analysis and Optimization," Aero No. 48-84, June 1984.